UDK 621.937:66.011
Original scientific article/Izvirni znanstveni članek

ISSN 1580-2949
MTAEC9, 58(4)443(2024)

MODELING OF THE CUTTING FORCES IN END MILLING OF A METALLIC MULTILAYER MATERIAL

MODELIRANJE REZALNIH SIL PRI ČELNEM REZKANJU KOVINSKEGA VEČPLASTNEGA MATERIALA

Uroš Župerl[1*], Miha Kovačič[2]

[1]University of Maribor, Faculty of mechanical engineering, Smetanova 17, 2000 Maribor, Slovenia
[2]Štore steel, Železarska cesta 3, 3220 Štore, University of Ljubljana, Faculty of mechanical engineering, Aškerčeva 6, 1000 Ljubljana, Slovenia

Prejem rokopisa – received: 2023-04-04; sprejem za objavo – accepted for publication: 2024-04-29

doi:10.17222/mit.2023.847

Multilayer metal materials are increasingly used by tool shops in the production of transfer tools for sheet-metal forming. In research, it is found that during the machining of these advanced materials, damage to the cutting edge often occurs due to jumps in the cutting forces. The size of the cutting forces when milling a multi-directionally layered metal material is influenced by both the direction of depositing the individual layer and the geometry of the cutting tool. The main goal of the research was to create a mechanistic model of cutting forces for the end-milling of unidirectional and multidirectional 20MnCr5/316L four-layered metal material. The results of the model were compared with experimental data, where a good agreement was found when milling unidirectional layered material and a slightly worse agreement when milling multidirectional material. The maximum observed deviation of the predicted cutting forces is 14.6 % for all the comparative tests.

Keywords: end-milling, metallic multilayer material, cutting forces, mechanistic model.

Večslojni kovinski materiali se vse bolj uporabljajo v orodjarnah pri izdelavi transfernih orodij za preoblikovanje pločevine. V raziskavah je bilo ugotovljeno, da pri obdelavi teh naprednih materialov pogosto pride do poškodbe rezalnega roba zaradi skokov rezalnih sil. Na velikost rezalnih sil pri rezkanju večsmerno nanešenih plasti kovinskega materiala vplivata tako smer nanosa posamezne plasti kot tudi geometrija rezalnega orodja. Glavni cilj raziskave je bil izdelati mehanistični model rezalnih sil za čelno rezkanje enosmernega in večsmernega štirislojnega kovinskega materiala 20MnCr5/316L. Rezultate modela smo primerjali z eksperimentalnimi podatki, kjer je bilo ugotovljeno dobro ujemanje pri rezkanju enosmernega plastnega materiala in nekoliko slabše ujemanje pri rezkanju večsmernega materiala. Največje opaženo odstopanje napovedanih rezalnih sil je bilo 14,6 % za vse izvedene primerjalne preizkuse.

Ključne besede: oblikovno frezanje, kovinski večplastni materiali, rezalne sile, mehanističen model.

1 INTRODUCTION

Multi-layer metal materials are increasingly used in the tool industry. Such materials are produced using the Laser Engineered Mesh Design (LENS) process.[1] The research[2] shows that the machinability of such material depends on the position of the workpiece in relation to the direction of movement of the tool. Machining such advanced materials is extremely challenging due to jumps in the cutting forces that cause excessive tool wear and tool damage.[3] Non-uniform magnitudes of the cutting forces lead to a deterioration of the quality of the machined surface; therefore, knowledge and control of the cutting forces is crucial to achieving the quality of machining.[4] There are many studies on the machinability of hard-to-machine nickel-based alloys,[5] titanium alloys[2] and composite materials.[6] In the literature, there are some studies on the machinability of difficult-to-machine aircraft alloys and composites,[3] titanium alloys,[2,7,8] Ni-based alloys[5] and composites.[6]

*Corresponding author's e-mail:
uros.zuperl@um.si (Uroš Župerl)

There are several mechanistic models[9] that consider tool wear,[10] tool deflection,[11] flank wear,[9] chip shape and size,[12] etc. In these models, the cutting forces are related to the thickness of the uncut chip and the specific cutting forces.[13] In the case of multidirectional layered materials, the determination of specific constants is even more challenging due to the different properties of the individual layers. Researchers predicted the cutting forces when milling layered laminates with different fibre directions.[6,14,15] A review of the literature shows that no work can be identified that considers the layer-cladding directions of multidirectional layered metal material in determining machinability.

Our contribution describes a mechanistic model of cutting forces in the helical end milling of layered metallic materials with unidirectional applied layers. A review of the literature showed that there is no evidence of work that attempts to model the cutting forces when milling multidirectional layered metal materials.

Excessive cutting tool wear occurs during the machining of such materials. Since tool wear is directly related to cutting forces, knowing precise cutting forces is critical for choosing optimal cutting conditions that result in longer tool life and reduced machining errors. Therefore, the main goal of the developed model of cutting forces is to evaluate the quality of machining and reduce the damage to cutting tools by accurately predicting the cutting forces.

The article is divided into 6 sections. Section 1 introduces the topic of multi-layer material machinability and the modelling of cutting forces in milling processes. Section 2 presents a mechanistic model for predicting the cutting forces in helical milling. Then follows a description of the experimental implementation and equipment. Section 4 presents the results of the developed model. Section 5 concludes the paper.

2 MECHANISTIC MODEL OF CUTTING FORCES

When predicting, the model considers the cutting parameters, the current angle of rotation of the milling tool and the direction of deposition of all the layers of the multi-layer material. In the mechanistic model, the cutter is cut into many very thin discs k. For each disc, the inclination angle is equal to the helix angle. The specific cutting force coefficients K_c and K_t are independent of the inclination angle in each disc and are determined based on an orthogonal milling test. The results of the orthogonal milling test are used to calculate K_c and K_t. The radial and tangential cutting forces are then calculated for each disc. By integrating the components of the cutting forces on all the disc's k that are in contact with the workpiece, the total cutting force on the tool is calculated.

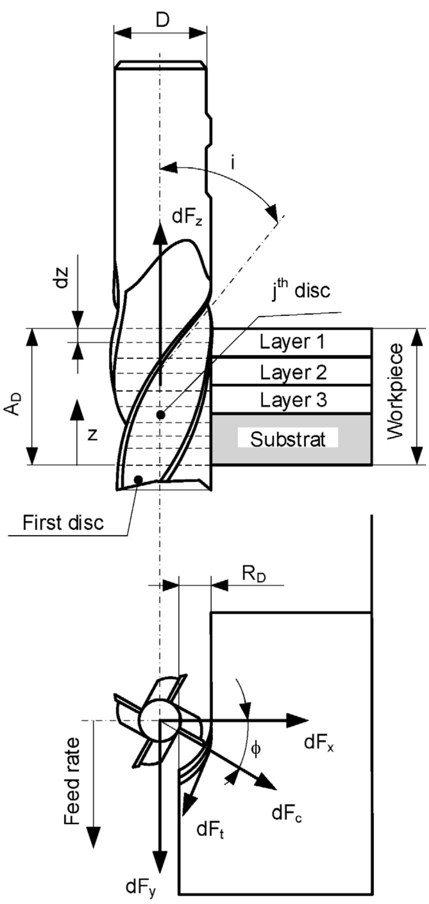

Figure 1: Scheme of the milling cutter and its breakdown into discs with marked cutting forces when milling multi-layer metal material

Figure 1 shows a milling cutter with helix angle i, diameter D and number of flutes N. On each differential disc in contact with the workpiece, forces $\mathrm{d}F_t$ and $\mathrm{d}F_c$ appear during cutting. These two forces are calculated as the product of the uncut chip thickness h_j, the axial depth of cut z and the value of the specific cutting forces according to Equation 1 and Equation 2, where dz is the height of the disc. The uncut chip thickness h_j of the disc j depends on the rotational frequency of the tool n_t, the feed speed of the tool f, and the engagement angle ϕ. The uncut chip thickness h_j is given by Equation 3.

$$\mathrm{d}F_c(\phi_j, z) = K_c \cdot h_j(\phi_j, z) \cdot \mathrm{d}z \tag{1}$$

$$\mathrm{d}F_t(\phi_j, z) = K_t \cdot h_j(\phi_j, z) \cdot \mathrm{d}z \tag{2}$$

$$h_j(\phi_j, z) = \frac{f}{n_t N} \cdot \sin\phi_j \tag{3}$$

The immersion angle for disk j on the flute n at the axial depth of cut z is given by Equation 4.

$$\phi_j(z) = \phi + n\frac{2\pi}{N} - \left(\frac{2\tan\beta}{D}\right)_j z; \quad n=0.1,...(n-1) \tag{4}$$

The axial component of the cutting force dF_a for the j-th disk is calculated by vector analysis with the help of dF_t and dF_c. The following formula is used for the calculation of dF_a, in which the inclination angle i, the normal rake angle α and the chip flow angle η are considered.

$$\mathrm{d}F_a(\phi_j, z) = \\ = \frac{\mathrm{d}F_c(\sin i - \cos i \cdot \sin\alpha \cdot \tan\eta) - \mathrm{d}F_t \cos\alpha \cdot \tan\eta}{\sin\beta \cdot \sin\alpha \cdot \tan\eta + \cos i} \tag{5}$$

The cutting forces $\mathrm{d}F_c$ and $\mathrm{d}F_t$ are transformed to the feed $\mathrm{d}F_y$ component and normal $\mathrm{d}F_x$ component using the following relations:

$$\mathrm{d}F_x(\phi_j, z) = \mathrm{d}F_t \cdot \cos\phi_j - \mathrm{d}F_c \cdot \sin\phi_j \tag{6}$$

$$\mathrm{d}F_y(\phi_j, z) = \mathrm{d}F_t \cdot \cos\phi_j + \mathrm{d}F_c \cdot \cos\phi_j \tag{7}$$

$$\mathrm{d}F_z(\phi_j, z) = \mathrm{d}F_a \tag{8}$$

The total cutting force on the tool is determined by the sum of the forces on the individual discs of the tool that are in contact with the workpiece. The axial cutting depth A_D and the number of cutting edges of the tool are considered in the calculation.

$$F_x = \sum_{n=0}^{N}\sum_{j=0}^{k} \mathrm{d}F_x \tag{9}$$

$$F_y = \sum_{n=0}^{N}\sum_{j=0}^{k} \mathrm{d}F_y \tag{10}$$

$$F_z = \sum_{n=0}^{N} \sum_{j=0}^{k} \mathrm{d}F_z \quad (11)$$

$$\psi_j = \begin{cases} \theta - \phi_j & 0 \le \phi_j < \theta \\ 180 - (\phi_j - \theta) & \phi_j > \theta \\ 180 - \theta & \theta = 0 \end{cases} \quad (12)$$

Table 1: Pseudo-code of the algorithm for simulating the cutting forces in helical milling.

Read_inputs	
Cutting condition	f, n_t, A_D, R_D
Helical cutter data	D, N, i
Specific cutting forces/layer	K_t, K_c
The angle of layer cladding	θ
No. of cutting disc	k
No. of cutting flutes	N
Write_outputs	
Cutting force/engagement angle	$F_y(\phi)$, $F_x(\phi)$, $F_z(\phi)$
Calculation_variables	
Calculation of tool feed	f
Setting the engagement angle	ϕ =0
If $\phi \le \phi_{exit}$	Engagement angle $0 \le \phi \le \phi_{exit}$
Calculation of radial chip thickness	$h(\phi)$
Set $F_x, F_y, F_z = 0$; $j=1$	
If $j \le k$	Integration loop from 0 to A_D
Determine engagement angle	ϕ
Recall K_t and K_c from ANFIS Calculation of differential forces	$dF_t(\phi, z)$, $dF_c(\phi, z)$ and $dF_a(\phi, z)$
Transformation of cutting force in *x-y-z* direction	$dF_y(\phi)$, $dF_x(\phi)$, $dF_z(\phi)$
Determination of cumulative force	$F_x(\phi)$, $F_x(\phi)$, $F_z(\phi)$
next j	$j = j + 1$
else.	
$\phi = \phi + 2\pi n\, t/60$; t [s]	
Plot $F_y(\phi)$, $F_x(\phi)$, $F_z(\phi)$	
else	
stop	
end	

The general pseudocode of the algorithm for the simulation of the cutting forces in the helical milling of multi-layered metal materials is presented in **Table 1**.

3 SPECIFIC CUTTING FORCES

In the research, layered metal materials are used, in which the layers have different machinability. This section describes the procedure for determining the specific cutting forces of unidirectional layered metal materials for a wide range of cladding directions and cutting parameters. Experimental data for determining the specific cutting forces were obtained from milling experiments in which several unidirectional layered materials were machined with different cutting parameters. The input vector of the database consists of the material cladding direction (ψ), cutting speed (n_t), feed rate (f) and chip thickness (h). Specific cutting forces K_c and K_t represent the output vector of the data base. The cutting forces measured in the experiments are used to calculate the specific cutting forces for a specific pair of tool and workpiece for several material-cladding directions and chip thickness. The layers of the individual workpieces were made with an equal direction of cladding. When determining the specific cutting forces K_c and K_t, the angle of layer deposition and the uncut thickness of the chip are considered. Therefore, in the specific cutting force determination, it is necessary to correct the normal rake angle with the effective cladding direction of the material gradient layer ψ_j, which is given by Equation 12. The angle of cladding of the gradient material layer is denoted by θ. The constant of the specific cutting force is calculated as the quotient between the measured component of the cutting force and the theoretical area of the uncut chip according to Equation 13.

$$\begin{aligned} K_t &= F_t(n_t, f, \psi, h) \cdot (A_D \cdot h(\phi))^{-1} \\ K_c &= F_c(n_t, f, \psi, h) \cdot (A_D \cdot h(\phi))^{-1} \end{aligned} \quad (13)$$

In the equation, F_t and F_c are obtained from measurements. The experimentally evaluated cutting forces F_x and F_y are first transformed into the tangential F_t and ra-

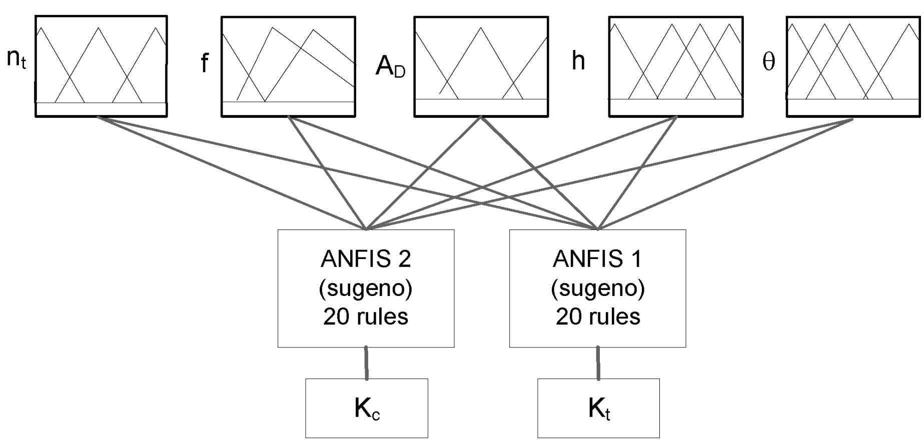

Figure 2: ANFIS structure for predicting the specific cutting forces K_c and K_t

dial cutting force F_c. Then, F_t and F_c are equated to analytically derived force expression, which leads to the identification of specific cutting forces. The expression in the denominator is the calculated area of the uncut chip. The instantaneous cross-section of the chip is determined by the product of the axial cutting depth A_D and the instantaneous radial thickness of the uncut chip h, which is formed at the engagement angle ϕ. The radial thickness of the uncut chip h is calculated using Equation 3, where f is the feed rate, n_t is the tool rotation frequency, and N is the number of tool blades. The values of n_t and f are determined according to the plan of experiments.

The experimental values of K_c and K_t were then used to build the ANFIS (adaptive neural inference system) predictive model of specific cutting forces. To train, test and validate the ANFIS model, 54 machining experiments were carried out. The machining experiments were carried out with three levels of tool rotation frequency, three levels of feed speed, two levels of axial depths of cut and three unidirectional workpiece configurations (three-layer cladding directions).

A total of 1080 data points obtained from experiments were used to create the ANFIS model. These data sets were randomly divided into a training/validation set (720 data points) and a testing set (360 data points). The ten-fold cross-validation was used to assess the accuracy of the developed ANFIS models. The results of the ten-fold cross-validation analysis show that the maximum prediction error of the ANFIS model is 5.02 % for K_c and 4.7% for K_t with a 95 % confidence interval. The predicted values of the K_c and K_t are in close agreement with the experimentally obtained values.

The developed ANFIS model generalizes K_c and K_t according to the cutting conditions that did not participate in the learning process of the model. The structure of the ANFIS model, which connects 5 inputs and 2 outputs with 40 logical rules, is shown in **Figure 2**.

4 EXPERIMENTAL EQUIPMENT AND PROCEDURE

Machining experiments to develop the mechanistic cutting-force model were carried on the Heller BEA02 machine tool. The workpieces in the machining experiments for the creation of the ANFIS model of specific cutting forces (3 workpieces) and for the validation of the mechanistic cutting force model are shown in **Figure 3**. **Table 2** shows the cutting conditions of 54 orthogonal milling experiments for the creation, testing and validation of the ANFIS model. A single flute carbide end mill with a diameter of 16 mm and a rake angle of 3.7° is used to determine K_t and K_c.

For the validation of the developed mechanistic model, four experiments were carried out with a segmented helical milling cutter with a diameter of 8 mm, two flutes, a helix angle of 25° and an inclination angle of 4.7°. The cutting conditions for the performed four

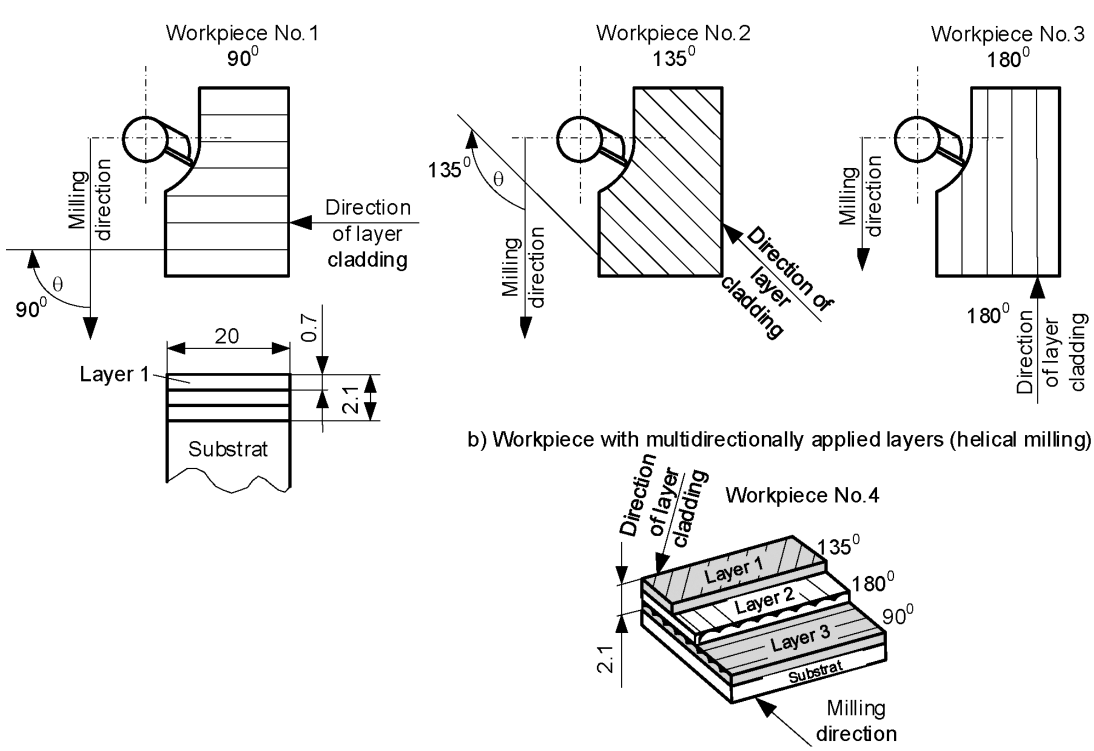

Figure 3: Placement of the workpieces in the experiments according to the milling direction

helical milling experiments are described in Table 2. One workpiece has three layers, which are applied at an angle of 90°, 135° and 180°. Layers have different machinability; this property of the material, expressed in the form of experimentally calculated specific cutting forces K_c and K_t, was considered when modelling the cutting forces. Therefore, the research devoted much work to determining the material coefficients for individual layers of multilayer material. The other three workpieces have three identical layers, which are made in the same cladding direction.

Table 2: Cutting conditions of the machining experiments with the indicated layer-cladding directions.

Variable	Orthogonal milling experiment	Helical milling experiment
n_t [min^{-1}]	3600, 3900, 4200	3900
f [m/min]	190, 240, 290	190
R_D [mm]	1.2	0.6
A_D [mm]	1.8, 2	2
D [mm]	16	6
Layer cladding direction θ [°]	90, 135, 180	90, 180, 135, 90/135/180
Number of flutes	1	2
Helix angle [°]	0	25.9
Radial angle [°]	3.7	5.1

The tool material is sintered tungsten carbide with a hardness of 1800 HV. Helical milling was performed on unidirectional and multidirectional workpieces with a tool rotation frequency of 3900 min^{-1}, a feed rate of 190 m/min, a depth of cut of 2 mm and a radial depth of cut of 0.6 mm. A Kistler piezoelectric dynamometer, a two-mode charge amplifier with a lowpass filter with a cut-off frequency of 2.5 kHz is used to measure the cutting forces.

A workpiece with a constant direction of the cladded layers, which are made of stainless steel 316L, is used. All three layers are made with the same cladding direction. The measured hardness of the manufactured layers is 288 HV. The tensile strength of the 315L material is 485 MPa. The basic substrate is made of 20MnCr5 with a tensile strength of 250 MPa and a measured hardness of 850 HV. In orthogonal milling, the tool feeding direction was at an angle of 90°, 135° and 180° with respect to the direction of layer cladding (**Figure 3a**). The workpiece for the helical milling test (**Figure 3b**) is made of the same subtract with three layers applied at an angle of 90°, 135° and 180° with respect to the tool feed direction.

5 RESULTS AND DISCUSSION

This section presents the results of four machining tests (**Table 2**; Helical milling experiments), which were carried out to validate the mechanistic model of cutting forces. Validation is performed by comparing the calculated values of the cutting forces with the signals of the measured cutting forces. For comparison, the values of the predicted and measured cutting force are graphically presented in the diagrams with respect to the engagement angle. From the diagrams, the agreement of the time course of the predicted cutting forces with the time course of the measured cutting forces was assessed. Finally, the maximum deviation between the model predictions and experimental values of the cutting forces in the milling of unidirectional and multidirectional workpieces was calculated.

Figure 4 shows the predicted and measured components of the cutting force depending on the angle of rotation of the tool when milling layered material. From the course of the cutting force, the maximum force can be seen at the 20° engagement angle. This is the maximum cutting force acting on one tooth of the tool during one revolution of the tool. The course of the cutting force is consistent with the increase in the thickness of the chip. When entering the material, the thickness of the chip is 0 and then increases to a maximum value just before the tooth exits the material. As the tool rotates, the angle between the blade and the cladding direction of the material layer changes. The results show that the largest jump in the cutting force occurs when milling multi-layer material with a 90° direction of layer cladding. This jump in cutting force is greater than the jump in cutting force when milling material with a 180° direction of layer cladding. In the case of material with a layer cladding angle between 90° and 135°, there is a noticeable increase in the magnitude of the cutting force. An increased fluctuation in force magnitude is also noticeable. The most unfavourable cutting conditions occur when milling material with a 135° layer cladding direction. Irregular chip shapes could be detected, which could be the result of the tip of the tooth sticking into the boundary space between the deposited layers. In the case of material with a layer cladding direction between 135°and 180°, there is a noticeable reduction in the magnitude of the cutting force. There is also less vibration. **Figures 4d** shows the measured and predicted cutting forces for the helical milling of workpieces with unidirectional applied layers. The course of the cutting force when milling a multidirectional workpiece has two peaks of the cutting force (**Figure 4d**). The two jumps of the cutting force coincide with the passage of the tool tooth over the junctions of different material layers with different cladding directions. In the experiment, the tool first processes the bottom layer, where the first peak of the cutting force components appears. It then hits the middle layer and eventually exits all three layers. When milling the middle layer with a 180° cladding direction, there is a noticeable reduction in the cutting force. A second jump in cutting force occurs when passing through all three layers. When processing the upper layer, chips of an unfavourable shape appear. The maximum cutting force occurs. The course of the cutting force depends on the thickness

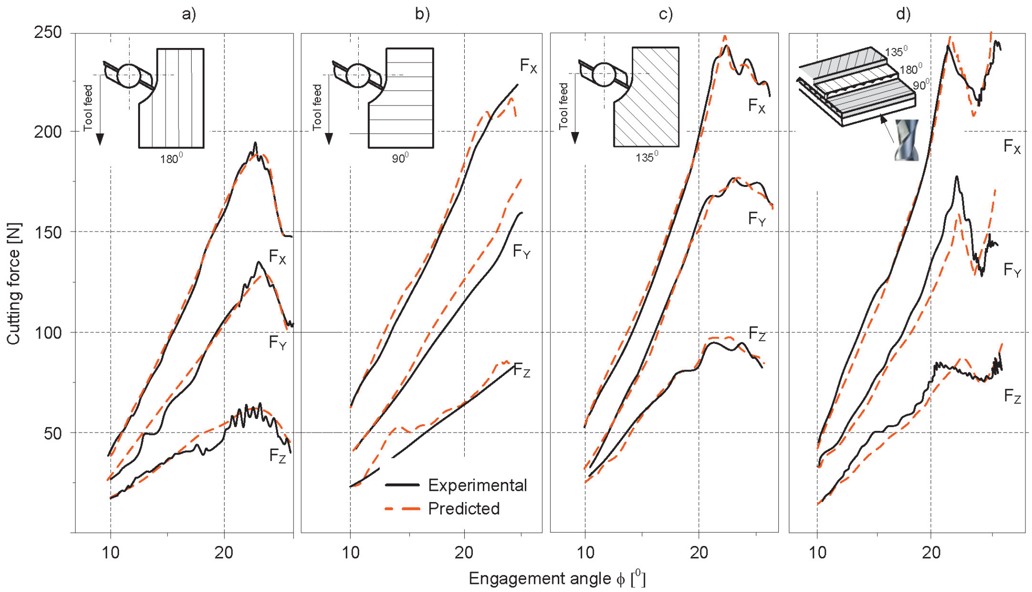

Figure 5: Predicted and measured cutting forces when milling unidirectional and multidirectional three-layer metal material: a) with 180° layer application direction b) with 90° layer application direction c) with 135° layer application d) with 135° /180° /135° layer application directions

of the applied layers and the sequence of layers with different cladding directions. The results in **Figure 4** shows that the developed model of cutting forces is effective in predicting the cutting forces depending on the engagement angle when milling multi-layered metal materials. The maximum error of the predicted forces is 7.8 % for the F_x force, 10.1 % for the F_y component and 14.6 % for the F_z component of the cutting force. The smallest error can be detected when processing a workpiece with a 90° direction of applied layers. The largest error of the model is when predicting the cutting forces for a workpiece with different directions of deposition for the individual layers.

6 CONCLUSION

The article presents a mechanistic cutting force model for the helical milling of layered metal materials. During the calculation, the model considers the machinability of each material layer, given by a specific cutting-force constant. The calculation of constants of specific cutting forces considers the direction of the layers deposition of multilayer metal material. By changing the material of the layer, it is necessary to perform three additional standard machining tests to determine the specific cutting forces for the three deposition directions of this layer. The large number of tests to obtain specific cutting forces for different combinations of materials and deposition directions represents the main challenge of this research. However, during the machining test and data acquisition, the ANFIS system automatically upgrades the predictive model of the specific cutting forces with new material data in a few seconds without using statistics and programming. By pressing a start button in the ANFIS software, the data from the experimental tests and the associated parameters are automatically classified into data sets for training and testing. Then, the training and validation of the ANFIS model are performed. The validated ANFIS model can then generalize the specific cutting force K_c and K_t for any current material layer deposition direction, making the method practical, widely applicable, and suitable for industrial use. Experimental testing established that the mechanistic cutting-force model is effective in predicting the flow of cutting forces in relation to the cutting parameters and the cladding direction of layers of the unidirectional and multidirectional 20MnCr5/316L four-layered material. An excellent agreement of the predicted forces with the measured ones is found for the workpieces with 180° and 135° directions of the cladded layers. A slightly worse match is found for workpieces with 90° direction of cladded layers. The maximum error of the predicted forces is 7.8 % for the F_x force, 10.1 % for the F_y component and 14.6 % for the F_z component of the cutting force. The largest error of the model is when predicting the cutting forces for a workpiece with different directions of deposition of individual layers.

7 REFERENCES

[1] E. R. I. Mahmoud, Characterizations of 304 stainless steel laser cladded with titanium carbide particles, Advances in Production Engineering & Management, 10 (**2015**) 6, 115–124, doi:10.14743/apem2015.3.196

[2] F. Hojati, A. Daneshi, B. Soltani, B. Azarhoushang, D. Biermann, Study on machinability of additively manufactured and conventional titanium alloys in micro-milling process, Precision Engineering, 62 (**2020**) 1–9, doi:10.1016/j.precisioneng.2019.11.002

[3] R. M'Saoubi, D. Axinte, S.L. Soo, C. Nobel, H. Attia, G. Kappmeyer, S. Engin, W.M. Sim, High performance cutting of advanced aerospace alloys and composite materials, CIRP Annals-Manufac-

turing Technology, 64 (**2015**) 2, 557–580, doi:10.1016/j.procir.2016.05.038

4 L. Yang, M.L. Zheng, Simulation and analysis of ball-end milling of panel moulds based on Deform 3D, International Journal of Simulation Modelling, 16 (**2017**) 2, 343–356, doi:10.2507/IJSIMM16(2)CO9

5 I. Tabernero, A. Lamikiz, S. Martínez, E. Ukar, J. Figueras, Evaluation of the mechanical properties of Inconel 718 components built by laser cladding, International Journal of Machine Tools and Manufacture, 51 (**2011**) 6, 465–470, doi:10.1016/j.ijmachtools.2011.02.003

6 J. Sheikh-Ahmad, Y. He, L. Qin, Cutting force prediction in milling CFRPs with complex cutter geometries, Journal of Manufacturing Processes, 45 (**2019**), 720–731, doi:10.1016/j.jmapro.2019.08.009

7 G. Bonaiti, P. Parenti, M. Annoni, S. Kapoor, Micro-milling Machinability of Additive Titanium Ti-6Al-4V, Procedia Manufacturing, 10 (**2017**) 497–509, doi:10.1016/j.promfg.2017.07.104

8 F. Montevecchi, N. Grossi, H. Takagi, A. Scippa, H. Sasahara, G. Campatelli, Cutting forces analysis in additive manufactured AISI H13 alloy, Procedia Cirp, 46 (**2016**), 476–479, doi:10.1016/j.procir.2016.04.034

9 G. Song, S. Sui, L. Tang, Precision prediction of cutting force in oblique cutting operation, The International Journal of Advanced Manufacturing Technology, 81 (**2015**) 1–4, 553–562

10 Y. Sun, Q. Guo, Numerical simulation and prediction of cutting forces in five-axis milling processes with cutter run-out, International Journal of Machine Tools and Manufacture, 51 (**2011**) 10–11, 806–815, doi:10.1016/j.ijmachtools.2011.07.003

11 O.E.E.K. Omar, T. El-Wardany, E. Ng, M.A. Elbestawi, An improved cutting force and surface topography prediction model in end milling, International Journal of Machine Tools and Manufacture, 47 (**2007**) 7–8, 1263–1275, doi:10.1016/j.ijmachtools.2006.08.021

12 S. Qu, J. Zhao, T. Wang, F. Tian, Improved method to predict cutting force in end milling considering cutting process dynamics, The International Journal of Advanced Manufacturing Technology, 78 (**2015**) 9–12, 1501–1510, doi:10.1007/s00170-014-6731-5

13 O. Tuysuz, Y. Altintas, H.Y. Feng, Prediction of cutting forces in three and five-axis ball-end milling with tool indentation effect, International Journal of Machine Tools and Manufacture, 66 (**2013**), 66–81, doi:10.1016/j.ijmachtools.2012.12.002

14 Y. Karpat, N. Polat, Mechanistic force modeling for milling of carbon fiber reinforced polymers with double helix tools, CIRP Annals, 62 (**2013**) 1, 95–98, doi:10.1016/j.cirp.2013.03.105

15 D. Kalla, J. Sheikh-Ahmad, J. Twomey, Prediction of cutting forces in helical end milling fiber reinforced polymers, International Journal of Machine Tools and Manufacture, 50 (**2010**) 10, 882–891, doi:10.1016/j.ijmachtools.2010.06.005